ACTA ACUSTICA UNITED WITH ACUSTICA
Vol. 97 (2011) 115 – 127
DOI 10.3813/AAA.918392

Explicit Analytical Representations in the Multiple High-Frequency Reflection of Acoustic Waves from Curved Surfaces: The Leading Asymptotic Term

Edoardo Scarpetta[1], Mezhlum A. Sumbatyan[2]
[1] D.I.I.M.A., University of Salerno, 84084 Fisciano (SA), Italy. scarpett@diima.unisa.it
[2] Faculty of Mathematics, Mechanics and Computer Science, Southern Federal University, Milchakova Street 8a, 344090 – Rostov-on-Don, Russia. sumbat@math.rsu.ru

Summary
In the context of wave propagation through a three-dimensional acoustic medium, we develop an analytical approach to study high-frequency diffraction by multiple reflections from curved surfaces of arbitrary shape. Following a previous paper (of one of us) devoted to two-dimensional problems, we combine some ideas of Kirchhoff's physical diffraction theory with the use of (multidimensional) asymptotic estimates for the arising diffraction integrals. Some concrete examples of single and double reflection are treated. The explicit formulas obtained by our approach are compared with known results from classical geometrical diffraction (or Ray-) theory, where this is applicable, and their precision is tested by a direct numerical solution of the corresponding diffraction integrals.

PACS no. 43.20.-f, 43.55.-n

1. Introduction

Diffraction theory in acoustics gives a bright example of combination between different approaches, namely, those based on heuristic methods with those constructed through strictly formal (mathematical) procedures. Many important and interesting solutions were originated from heuristic ideas - like Huygens-Fresnel principle, Fermat principle, etc. - giving even rise to well-known classical theories. In this context, the most impressive one is in fact the Kirchhoff's physical diffraction theory, which is based upon a clear "light and shadow" concept for diffracted wave fields. On the other hand, strict mathematical methods did also yield significant progresses in the development of correct solutions, different sometimes from those predicted by the common intuition.

The background of diffraction theory was laid by the founders of the modern mathematical physics: a good survey can be found in [1, 2]. Some interesting analytical representations were developed for diffraction by obstacles with smooth convex boundaries (as well as by thin screens) in the high-frequency range, which is important for many practical applications, including Room Acoustics. However, asymptotic results like these show poor precision in border domains, such as semi-shadow, caustics, etc. Moreover, they generally involve only the leading asymptotic term of the amplitude for the diffracted wave.

Recently, the rapid progress in computer science led to an absolutely new approach based on direct numerical treatments of the diffraction problems. When implemented on appropriate computers, this approach allows one to obtain numerical results with any desirable precision. However, in the high-frequency range for three-dimensional problems, such an approach leads, as a rule, to huge algebraic systems which cannot be treated in real time even by the use of modern computers. In fact, to obtain reliable results by any grid numerical method, one has to take at least 10 nodes per wavelength; if one takes the frequency band $f = 2$ kHz, whose wavelength in air is 17 cm, then in a room of average size 17 m one must apply at least 1000 nodes along the room length. In a three-dimensional problem, this will result in $10^8 - 10^9$ nodes in the room, a too large dimension even for powerful super computers.

Thus, having realized that a direct numerical simulation cannot provide real-time computations, many researchers proposed various combinations of numerical and heuristic approaches. This gave rise to a number of theories, but only two of them showed good practical properties when implemented on computers. These are those based on Virtual Image and Ray Tracing methods [3, 4, 5]. Leaving to such references the description of the former, we turn our attention to the latter one which is rather involved in this paper.

Received 26 March 2010,
accepted 23 October 2010.

The Ray (Tracing) method in acoustics was proposed on the basis of a certain physical analogy with the propagation of light rays; the corresponding theory is also referred to as "geometrical diffraction theory". In the case of multiple reflection, the propagation is traced sequentially from one reflection to another, each one obeying to the specular (*mirror*) reflection geometric law. Generally, Ray method gives answer to the two basic questions: (i) what is the trajectory of the acoustic ray in the multiple reflection process? (the same of the light ray) (ii) what is the amplitude at the final receiving point? In the case where all reflectors are plane and acoustically rigid, such an amplitude is assumed to be the same as in the case of no reflection, when the distance between source and receiver is taken as the full path of ray's travel. Really, in the sense of mathematical justification, this simple idea has been proved strictly only for the case of single reflection from a plane surface, giving such a result through the leading high-frequency asymptotic term. Nobody proved this statement neither for multiple reflections, even when all reflectors are plane, nor in the case where the ray may change - after some reflection - the plane of its propagation. Moreover, even assuming the ray geometrical scheme for an arbitrary geometry, nobody knows what is the amplitude of the multiply reflected ray if at least one reflecting surface is curved. Following the basic idea of the Ray method [6, 7], the amplitude of the wave ray arriving at the receiver is defined by the geometry of the beam's cone-tube surrounding the ray's trajectory, when the ray is irradiated from the source. Obviously, after each reflection, the cone modifies its geometry, and this change depends upon the geometry of the current reflecting surface, as well as upon that of previous and next ones.

Giving a short review on Ray reflection from curved surfaces, let us note that, for a smooth convex reflecting shape, it is strictly derived a high-frequency asymptotic result in the case of single reflection [7]. This result contains the angle of incidence, the distances from the source and receiver to the reflecting point, as well as the two principal curvatures of the surface at the reflecting point. The respective formula, which is based indeed on the change of geometry of the beam's cone, gives an explicit expression for the reflected amplitude at some receiving point x, as follows [7]:

$$p_{ray}(x) \sim \exp\left[ik(L+L_0)\right]\left[(L+L_0)^2 + 2LL_0(L+L_0) \cdot \frac{k_1 \sin^2\beta + k_2 \sin^2\alpha}{\cos\gamma} + 4L^2L_0^2K^2\right]^{-1/2}, \quad (1)$$

where $k = \omega/c$ $(\to \infty)$ is the wave number, L_0 and L are the distances of the source and receiver, respectively, from the reflecting point, k_1 and k_2 the principal curvatures at the reflecting point, $K \equiv k_1 k_2$ the Gaussian curvature. A local Cartesian coordinate system is chosen on the surface with its center at the reflecting point, two coordinate axes along k_1 and k_2 and the third axis along the outer normal. The unit vector along the incident ray is $\{-\cos\alpha, -\cos\beta, -\cos\gamma\}$, the unit vector along the reflected ray is $\{-\cos\alpha, -\cos\beta, \cos\gamma\}$.

Such a formula cannot be extended neither to concave surfaces nor to the case of multiple reflections. We thus can conclude that, even for the double reflection from arbitrary smooth surfaces, there are no results of general kind, so that the most interesting cases, particularly for Room Acoustics applications, need a special investigation.

Other important approaches to high-frequency diffraction problems can be found in [8, 9, 10, 11, 12, 13, 14, 15]. Note that we don't pay attention to papers in which non-plane surfaces are approximated by a number of plane facets, since the correctness of such a simulation is very doubtful: indeed, as just noticed, even for single reflection the reflected amplitude contains the principal curvatures at the reflecting point; hence, putting these curvatures equal to zero cannot produce correct results. The same for papers which propose direct or quasi-direct numerical simulations, even if the suggested algorithms can significantly reduce the size of the resulting algebraic system. This is because the efficiency of such procedures fails in any case with the frequency increasing, and thus their results cannot be useful for the problems here considered.

In order to set up a strict general theory for (high-frequency) multiple reflections, one of us developed a new approach which combines certain ideas of Kirchhoff's physical diffraction theory with the use of multidimensional asymptotic estimates for some arising *diffraction integrals*, in the case of two-dimensional problems [16]. The main goal of the present work is to develop an analogous approach for three-dimensional (3-d) problems, where much more difficulties are involved.

At the end of this introduction, it should be noted that, aiming to improve its precision, some authors construct a correction of the Ray theory by adding to the ray-reflected amplitude also the contribution of the wave diffracted on the boundary (edges) of the surface [17]. The question is outside the goals of this paper, but the authors plan to devote their next efforts to study such a very interesting matter.

2. The Basics of the Proposed Method

As just stated, in this paper we aim to propose an analytical approach which leads to clear explicit formulas for high-frequency 3-d diffraction by obstacles with multiple reflections. This approach, arising in the ambit of Kirchhoff's physical diffraction theory, will yield the leading asymptotic term with the frequency increasing. Another goal is to test the precision of such analytical representations by a direct numerical treatment of the corresponding diffraction integrals.

So, let us start from the foundations of the quoted Kirchhoff theory. This is interpreted in different ways by different authors; thus, we give a certain view that may be different from other interpretations. The theory is based

ACTA ACUSTICA UNITED WITH ACUSTICA
Vol. 97 (2011)

on the following hypotheses which are valid for high frequencies, acoustically hard surfaces, and smooth convex obstacles (no repeated reflections), see Figure 1:

1. If the obstacle is convex, then its full boundary surface S consists of two different parts S^+ and S^- called respectively as "light" and "shadow" zones. The formal definition is as follows: if any finite-length line segment connecting source x_0 and arbitrary point $y \in S$ does not intersect any other part of S, then this point belongs to S^+. Otherwise, it belongs to S^-.
2. Full acoustic pressure in the shadow zone S^- is trivial: $p(y) = 0,\ y \in S^-$.
3. The diffraction in a small vicinity of any point in the light zone S^+ happens so as it would happen if the incident wave would be plane.
4. The diffraction in a small vicinity of any point y in the light zone S^+ happens so as it would happen in the problem of reflection of a plane incident wave from a semi-space whose boundary plane is tangential to S at point y.

As is known [5], these hypotheses imply an explicit definition of the full pressure $p(y)$ in the light zone: if we denote by $p^{inc}(y)$ the wave incident on surface S from some source, it holds

$$p(y) = 2p^{inc}(y), \quad y \in S^+. \tag{2}$$

It can be proved as a mathematical theorem that this Kirchhoff's prediction coincides with the leading asymptotic term at any fixed point $y \in S^+$, as frequency goes to infinity [18]. We are assuming a time dependence of harmonic type, omitting henceforth the corresponding factor $\exp(-i\omega t)$, $\omega = kc$ where k and c are wave number and wave speed, respectively.

Now, we can apply the exact form of the Kirchhoff-Helmholtz integral to get the scattered wave field at any receiving point [5]:

$$\begin{aligned} p^{sc}(x) &= \int_S \left[p(y)\frac{\partial\Phi(y,x)}{\partial n_y} - \frac{\partial p(y)}{\partial n_y}\Phi(y,x)\right] \mathrm{d}S \\ &= \int_{S^+} p(y)\frac{\partial\Phi(y,x)}{\partial n_y}\,\mathrm{d}S \\ &= \int_{S^+} 2p^{inc}(y)\frac{\partial\Phi(y,x)}{\partial n_y}\,\mathrm{d}S, \\ \Phi(y,x) &= \frac{\mathrm{e}^{ik|y-x|}}{4\pi|y-x|}, \end{aligned} \tag{3}$$

where we have used the boundary condition for acoustically hard surface: $\partial p/\partial n|_S = 0$. In equation (3), $\vec{n}_y$ is the outer unit normal to surface S at point $y \in S$ (see Figure 1), and $\Phi(y,x)$ is the (3-d) Green's function.

Now, let us assume a number of sequential multiple reflections from (smooth) curved surfaces $S_1, S_2, \ldots S_N$; see Figure 2. Following the Kirchhoff-Helmholtz integral representation, with the above boundary condition, we can write the scattered field at the final receiving point as

$$p^{sc}(x) = \int_{S_N^+} p(y)\frac{\partial\Phi(y,x)}{\partial n_y}\,\mathrm{d}S_N. \tag{4}$$

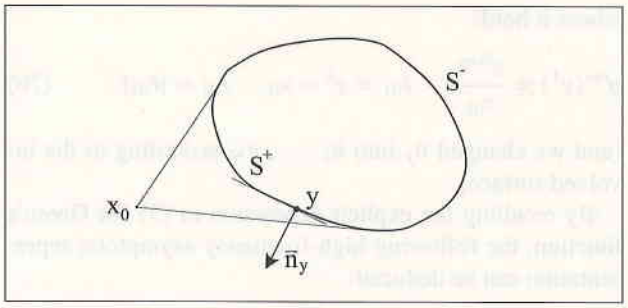

Figure 1. The sketch for Kirchhoff's physical diffraction theory.

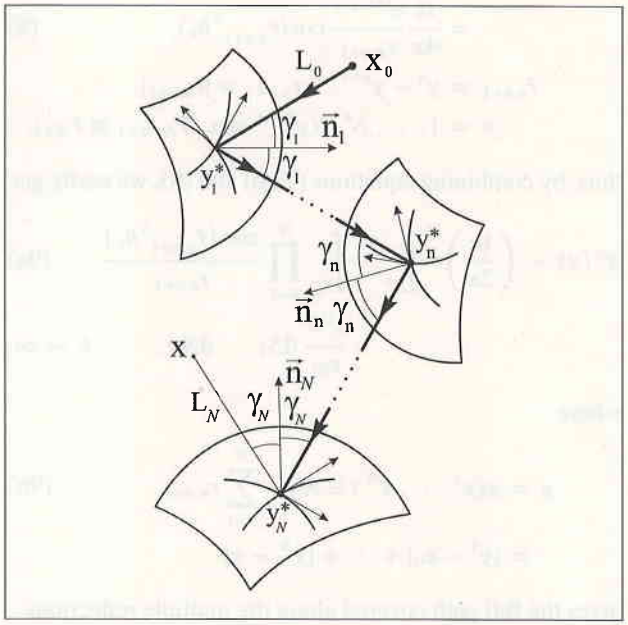

Figure 2. Sequential multiple reflection from an array of curved reflectors.

However, by analogy to what is done in (3), the value $p(y)$, $y \in S_N^+$, which gives the acoustic pressure on the N-th reflecting surface, is twice the value at the same points y as it would be if the surface S_N^+ would be absent, namely, twice the value of a wave field "incident" onto the surface S_N^+ for reflection from the (points of) surface S_{N-1}^+:

$$p^{sc}(x) = \int_{S_N^+} 2p(y^N)\frac{\partial\Phi(y^N,x)}{\partial n_N}\,\mathrm{d}S_N. \tag{5}$$

Henceforth, y^n $(n = 1, \ldots, N)$ denotes the points on S_n. By the same analogy, one can evaluate that

$$p(y^N) = \int_{S_{N-1}^+} 2p(y^{N-1})\frac{\partial\Phi(y^{N-1},y^N)}{\partial n_{N-1}}\,\mathrm{d}S_{N-1}, \tag{6}$$

and so on. As a consequence, by collecting all integrals together, we obtain

$$\begin{aligned} p^{sc}(x) = 2^N \int_{S_1^+} \cdots \int_{S_N^+} & p^{inc}(y^1)\frac{\partial\Phi(y^1,y^2)}{\partial n_1} \\ & \cdots \frac{\partial\Phi(y^N,x)}{\partial n_N}\,\mathrm{d}S_1 \ldots \mathrm{d}S_N, \end{aligned} \tag{7a}$$

where it holds

$$p^{inc}(y^1) = \frac{e^{ikr_{01}}}{r_{01}}, \quad \bar{r}_{01} = y^1 - x_0, \quad r_{01} = |\bar{r}_{01}| \tag{7b}$$

(and we changed $\bar{n}_y$ into $\bar{n}_1, \ldots, \bar{n}_N$ according to the involved surface).

By recalling the explicit expression in (3) for Green's function, the following high-frequency asymptotic representation can be deduced:

$$\frac{\partial \Phi(y^n, y^{n+1})}{\partial n_n} \sim ik\Phi(y^n, y^{n+1}) \cos\left(\bar{r}_{n,n+1} \hat{} \bar{n}_n\right) = \frac{ik}{4\pi} \frac{e^{ikr_{n,n+1}}}{r_{n,n+1}} \cos(\bar{r}_{n,n+1} \hat{} \bar{n}_n), \tag{8}$$

$$\bar{r}_{n,n+1} = y^n - y^{n+1}, \quad r_{n,n+1} = |\bar{r}_{n,n+1}|, \quad n = 1, \ldots, N \quad (y^{N+1} \equiv x, \ \bar{r}_{N,N+1} \equiv \bar{r}_{Nx});$$

thus, by combining equations (7a,b) and (8), we easily get

$$p^{sc}(x) \sim \left(\frac{ik}{2\pi}\right)^N \int_{S_1^+} \cdots \int_{S_N^+} \prod_{n=1}^{N} \frac{\cos\left(\bar{r}_{n,n+1} \hat{} \bar{n}_n\right)}{r_{n,n+1}} \cdot \frac{e^{ikg}}{r_{01}} \, dS_1 \ldots dS_N, \quad k \to \infty, \tag{9a}$$

where

$$g = g(y^1, \ldots, y^N) \equiv r_{01} + \sum_{n=1}^{N} r_{n,n+1} = |y^1 - x_0| + \cdots + |y^N - x| \tag{9b}$$

gives the full path covered along the multiple reflections.

Further simplification for equation (7a) can be found by applying a high-frequency estimate to the (multiple) *diffraction integral* in equation (9a,b). In this connection, the principal contribution to the leading asymptotic term is given by the *stationary point* according to the following representation holding for any M-fold integral taken over some domain Ω [19],

$$\int_\Omega f(y) e^{ikg(y)} \, dy \sim \left(\frac{2\pi}{k}\right)^{M/2} \exp\left[ikg(y^*) + \frac{\pi i}{4} \operatorname{sign} g''_{yy}(y^*)\right] \cdot \frac{f(y^*)}{\left|\det g''_{yy}(y^*)\right|^{1/2}} \quad (k \to \infty), \tag{10}$$

$$y = (y_1, \ldots, y_M), \qquad dy = dy_1 \ldots dy_M.$$

Here y^* denotes the so-called *stationary point*, namely, a (M-valued) point at which the *phase function* $g(y)$ has vanishing gradient,

$$\frac{\partial g(y^*)}{\partial y_1} = \cdots = \frac{\partial g(y^*)}{\partial y_M} = 0, \tag{11}$$

g''_{yy} is the Hessian matrix of function g :

$$g''_{yy} = \left\{\frac{\partial^2 g}{\partial y_m \partial y_\mu}\right\}, \quad m, \mu = 1, \ldots, M. \tag{12}$$

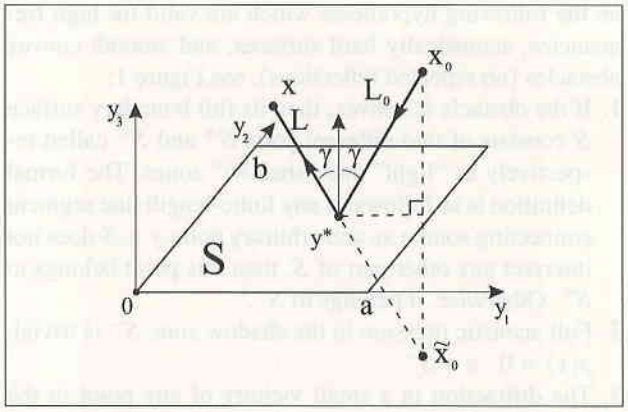

Figure 3. Single reflection from a plane rectangular screen.

sign g''_{yy} is the sign of Hessian, i.e. the difference between the number of its positive and negative eigenvalues, and finally $\det g''_{yy}$ is its determinant ($g''_{yy}(y^*) \equiv g''_*$).
In the forthcoming examples, the geometrical points on the reflecting surfaces corresponding to the values $y_1^*, \ldots, y_M^*$, will also be referred to as *stationary points*.
Thus, the novelty of our approach for 3-d problems consists in the derivation of the quoted diffraction integral along with the method of solving it (asymptotically) given by formula (10).

3. Examples on Single Reflection from Flat and Spherical Surfaces

3.1. Let us first consider the classical high-frequency diffraction by a plane rectangular (rigid) screen S of size $a \times b$, only to show the details of the mathematical technique proposed in this paper, which will be then extended to more complex geometries.

The geometry of the problem is shown in Figure 3. If $x_0 = (\xi_0, \eta_0, \zeta_0)$ is the source point and $x = (\xi, \eta, \zeta)$ the receiver point, the leading asymptotic term can be constructed by the geometrical diffraction (or Ray-)theory, which in this simple example amounts to introduce the virtual source $\tilde{x}_0 = (\xi_0, \eta_0, -\zeta_0)$ symmetric to the real one x_0 with respect to the reflection plane $y_3 = 0$, and to consider the full path of the ray from $\tilde{x}_0$ to x. It is interesting to verify whether this result can also be obtained by using equations (9a,b) and (10) in the ambit of our approach.

In this case, it holds $N = 1$ ($S_1 = S$), $y^1 \equiv y = (y_1, y_2, 0)$, $\bar{n}_1 = \{0, 0, 1\}$ and $\cos\left(\bar{r}_{1x} \hat{} \bar{n}_1\right) = -\zeta / r_{1x}$. Hence, equation (9a,b) for the amplitude of the reflected wave becomes

$$p^{sc}(x) \sim -\frac{ik\zeta}{2\pi} \int_S \frac{e^{ikg(y_1, y_2)} \, dy_1 \, dy_2}{\psi^2(y_1, y_2)\varphi(y_1, y_2)}, \quad k \to \infty, \tag{13a}$$

where we put

$$r_{01} = \left[(y_1 - \xi_0)^2 + (y_2 - \eta_0)^2 + \zeta_0^2\right]^{1/2} \equiv \varphi(y_1, y_2),$$
$$r_{1x} = \left[(y_1 - \xi)^2 + (y_2 - \eta)^2 + \zeta^2\right]^{1/2} \equiv \psi(y_1, y_2), \tag{13b}$$
$$g = \psi + \varphi.$$

It is evident that condition (11) for the stationary point leads to the systems

$$\begin{cases} \dfrac{y_1-\xi}{\psi}+\dfrac{y_1-\xi_0}{\varphi}=0 \\ \dfrac{y_2-\eta}{\psi}+\dfrac{y_2-\eta_0}{\varphi}=0 \end{cases} \Rightarrow \begin{cases} (y_1-\xi)^2\varphi^2=(y_1-\xi_0)^2\psi^2 \\ (y_2-\eta)^2\varphi^2=(y_2-\eta_0)^2\psi^2 \end{cases} \Rightarrow \begin{cases} (y_1-\xi)^2\zeta_0^2=(y_1-\xi_0)^2\zeta^2 \\ (y_2-\eta)^2\zeta_0^2=(y_2-\eta_0)^2\zeta^2 \end{cases}. \tag{14}$$

It follows from the first system above that differences $(y_1-\xi)$ and $(y_2-\eta)$ have opposite signs with respect to $(y_1-\xi_0)$ and $(y_2-\eta_0)$; therefore, the last system in (14) yields

$$\begin{cases} (y_1-\xi)\zeta_0=(\xi_0-y_1)\zeta \\ (y_2-\eta)\zeta_0=(\eta_0-y_2)\zeta \end{cases}, \tag{15}$$

whence the stationary point $y^*=(y_1^*, y_2^*, 0)$ is easily deduced as

$$y_1^*=\frac{\xi\zeta_0+\zeta\xi_0}{\zeta_0+\zeta}, \quad y_2^*=\frac{\eta\zeta_0+\zeta\eta_0}{\zeta_0+\zeta}. \tag{16}$$

Of course, further results are valid only if this point belongs to the reflection area, i.e., if $y^*\in S$. Note that, as expected, y^* coincides with the point of mirror reflection between x_0 and x.

Let us introduce the distances $L\equiv\psi|_{y^*}=\psi(y_1^*, y_2^*)$, $L_0\equiv\varphi|_{y^*}=\varphi(y_1^*, y_2^*)$ and the incident angle $\gamma=\pi-(\bar r_{01}\wedge\bar n_1)$. By the systems in (14), we get $\zeta_0^2L^2=\zeta^2L_0^2$, and thus

$$\frac{\zeta_0}{L_0}=\frac{\zeta}{L}=\cos\gamma, \tag{17}$$

which implies the well-known law of equality between reflection and incident angles (actually, a consequence of the stationarity condition); see Figure 3.

The Hessian is calculated directly as

$$g_*''=\begin{pmatrix} \dfrac{\partial^2 g}{\partial y_1^2} & \dfrac{\partial^2 g}{\partial y_1\partial y_2} \\ \dfrac{\partial^2 g}{\partial y_1\partial y_2} & \dfrac{\partial^2 g}{\partial y_2^2} \end{pmatrix}_{y=y^*}, \tag{18a}$$

where

$$\left.\frac{\partial^2 g}{\partial y_1^2}\right|_{y=y^*}=\frac{1}{L}\left[1-\frac{(y_1^*-\xi)^2}{L^2}\right]+\frac{1}{L_0}\left[1-\frac{(y_1^*-\xi_0)^2}{L_0^2}\right],$$

$$\left.\frac{\partial^2 g}{\partial y_2^2}\right|_{y=y^*}=\frac{1}{L}\left[1-\frac{(y_2^*-\eta)^2}{L^2}\right]+\frac{1}{L_0}\left[1-\frac{(y_2^*-\eta_0)^2}{L_0^2}\right], \tag{18b}$$

$$\left.\frac{\partial^2 g}{\partial y_1\partial y_2}\right|_{y=y^*}=-\frac{(y_1^*-\xi)(y_2^*-\eta)}{L^3}-\frac{(y_1^*-\xi_0)(y_2^*-\eta_0)}{L_0^3}.$$

Its determinant, after some transformations, turns out to hold

$$\det g_*''=\frac{\zeta^2(L+L_0)^2}{L^4L_0^2}. \tag{19}$$

In order to calculate the sign of the Hessian, we use the Sylvester criterium [20]: any symmetric matrix, whose all principal determinants are positive, is positive-definite. Our Hessian has only two principal determinants: the full determinant itself, equatin (19), and the element $\partial^2 g/\partial y_1^2$ given in equation (18b). The former is evidently positive; the latter is positive too since $L>|y_1-\xi|$ and $L_0>|y_1-\xi_0|$. If the Hessian is positive-definite, then all its (two) eigenvalues are positive, hence sign $g_*''=2$ in equation (10).

Now, let us calculate the integral in (13a,b) by means of equation (10) with $M=2$, $\Omega=S$ (the rectangle) and $f\equiv 1/(\psi^2\varphi)$. By collecting all results obtained, we get

$$p^{sc}(x)\sim\left(-\frac{ik\zeta}{2\pi}\right)\left(\frac{2\pi}{k}\right)\frac{e^{i[k(L+L_0)+\pi/2]}}{L^2L_0[\det g_{yy}''(y^*)]^{1/2}}=\frac{e^{ik(L+L_0)}}{L+L_0}, \quad k\to\infty. \tag{20}$$

Such a formula expresses just what Ray theory implies, and we aimed to verify; cf. also with equation (1) on putting $k_1=k_2=0$.

It should be noted that this result is free of the size of the reflecting surface - parameters a and b - that seems to be strange at first sight. Really, a more precise asymptotic representation should include further terms in the asymptotic expansion. As can be proved in the ambit of Ray theory, the contribution of the second (after the leading) asymptotic term would complete the above formula as follows:

$$p^{sc}(x)\sim\frac{e^{ik(L+L_0)}}{L+L_0}\left[1+O(1/k)\right], \quad k\to\infty. \tag{21}$$

However, the principal contribution is brought by the stationary points of the boundary edges, if there are any [17]. If this contribution would be taken into account, then the asymptotic estimate in the square bracket of equation (21) would be written as follows: $[1+O(1/k^{1/2})]$. All that is clearly shown by Figures 4a,b,c, where we compare the

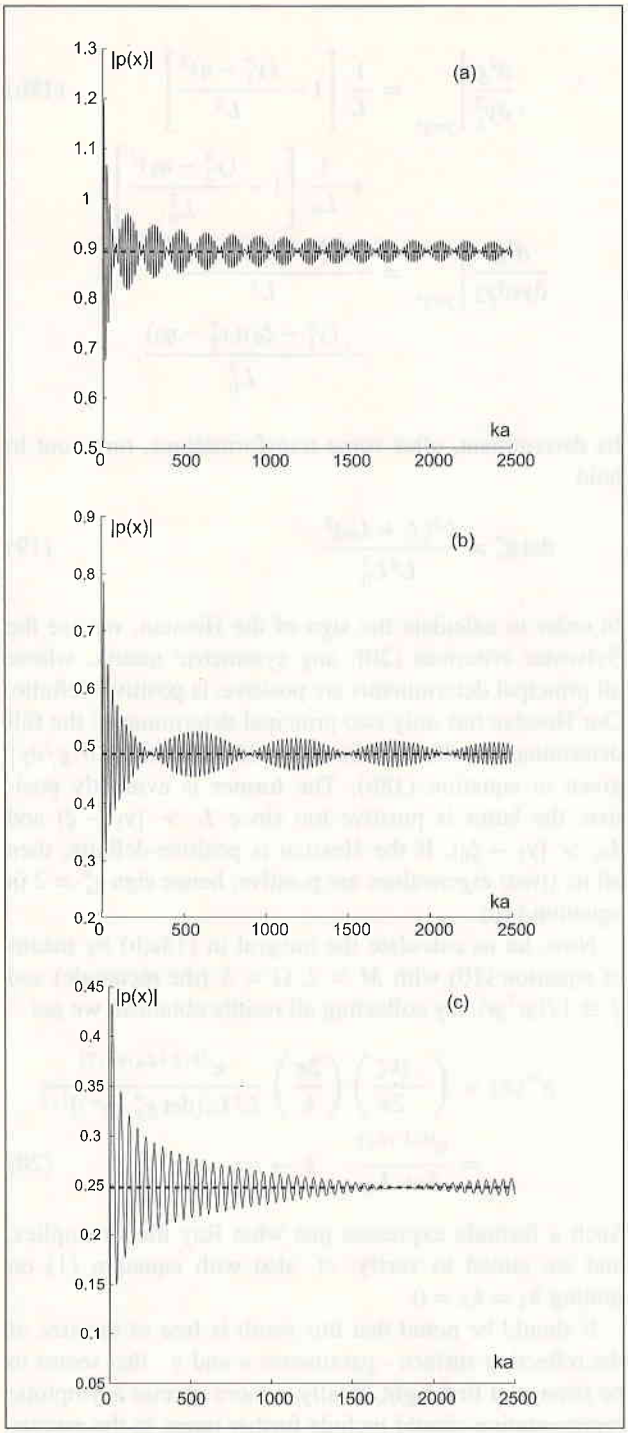

Figure 4. a,b,c. Comparison between Ray-theory prediction (21) (dashed line) and exact numerical calculation of integral (13a,b) (solid line): plane reflector, $a = b$, $\xi_0 = 0.75\,a$, $\xi = 0.25\,a$, $\eta_0 = \eta = 0.5\,a$ (a): $\zeta = \zeta_0 = 0.5\,a$, $\gamma = \arctan(1/2) \simeq 26.5^o$ (b): $\zeta = \zeta_0 = a$, $\gamma = \arctan(1/4) \simeq 14^o$ (c): $\zeta = \zeta_0 = 2a$, $\gamma = \arctan(1/8) \simeq 7^o$.

asymptotic result (21) with a direct numerical calculation of integral (13a,b) (which reflects the Kirchooff diffraction theory). For all three cases considered, the stationary (reflecting) point is located at the center of the square: $y_1^* = y_2^* = 0.5\,a$.

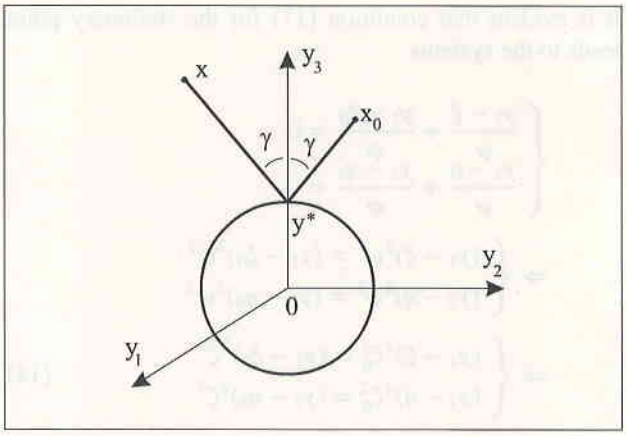

Figure 5. Single reflection from a spherical surface.

It is obvious that the difference between geometrical (Ray) and physical (Kirchhoff) diffraction theories decreases with the frequency parameter increasing. However, this approaching is very slow when frequency grows, that conform to the slow decay of the asymptotic estimate $O(1/k^{1/2})$ for $k \to \infty$.

3.2. The next example we consider here is a (non-symmetric) single reflection from a sphere of radius a; see Figure 5. Such a case can still be studied in the ambit of Ray theory, by equation (1); let us see whether it can be as well studied by the method proposed here.

It is evident that for arbitrary two points x and x_0 in the space, the coordinate system can be chosen so that both of them are located in the (vertical) plane $y_1 = 0$. The axis y_3 is taken so as to contain the mirror reflection point $\tilde{y}$: $\tilde{y} = (0, 0, a)$. So, let us put $x = (0, \eta, \zeta)$, $x_0 = (0, \eta_0, \zeta_0)$. In this case, one should substitute into equation (9a,b), where only one surface $S_1 = S$ remains and $y^1 \equiv y = (y_1, y_2, y_3 = \sqrt{a^2 - y_1^2 - y_2^2})$, the expressions

$$r_{1x} = \left[y_1^2 + (y_2 - \eta)^2 + \left(\sqrt{a^2 - y_1^2 - y_2^2} - \zeta \right)^2 \right]^{1/2} \equiv \psi(y_1, y_2),$$

$$r_{01} = \left[y_1^2 + (y_2 - \eta_0)^2 + \left(\sqrt{a^2 - y_1^2 - y_2^2} - \zeta_0 \right)^2 \right]^{1/2} \equiv \varphi(y_1, y_2), \tag{22}$$

$$g = \psi + \varphi, \quad \bar{n}_1 = \left\{ \frac{y_1}{a}, \frac{y_2}{a}, \frac{y_3}{a} \right\},$$

$$\mathrm{d}S = \frac{a}{y_3}\,\mathrm{d}y_1\,\mathrm{d}y_2,$$

$$\cos\left(\bar{r}_{1x} \overset{\wedge}{} \bar{n}_1\right) = (\bar{r}_{1x}/\psi) \cdot \bar{n}_1 = \frac{a^2 - (y_2\eta + y_3\zeta)}{a\,\psi(y_1, y_2)}.$$

After that, equation (9a,b) for the reflected amplitude becomes

$$p^{sc}(x) \underset{k \to \infty}{\sim} \frac{ik}{2\pi} \int_{S^+} \frac{\left[a^2 - (y_2\eta + y_3\zeta)\right] \mathrm{e}^{ikg(y_1, y_2)}}{y_3\,\psi^2(y_1, y_2)\,\varphi(y_1, y_2)}\,\mathrm{d}y_1\,\mathrm{d}y_2, \tag{23}$$

(where not specified, it holds $y_3 = \sqrt{a^2 - y_1^2 - y_2^2}$). As made before, let us now estimate this expression, as $k \to \infty$, by the use of equation (10). Since the phase function $g(y_1, y_2)$ in (22) is even with respect to y_1, it is clear that $\partial g/\partial y_1 = 0$ when $y_1 = 0$, so that for the stationary point it holds $y_1^* = 0$. Moreover, on putting

$$\frac{\partial g}{\partial y_2} = \frac{\zeta\, y_2/\sqrt{a^2 - y_2^2} - \eta}{\psi} + \frac{\zeta_0\, y_2/\sqrt{a^2 - y_2^2} - \eta_0}{\varphi} = 0 \quad (\text{at } y_1 = y_1^* = 0), \tag{24}$$

it can be seen from Figure 5 that the chosen coordinate system provides the equality $\eta/\psi = -\eta_0/\varphi$, and thus we deduce that $y_2 = 0 \equiv y_2^*$ solves equation (24). Therefore, the stationary point is $y^* = \tilde{y} = (0, 0, a)$ (see the comment after equation 17).

Let us calculate the Hessian and its determinant. After introducing the distances

$$L \equiv \psi\big|_{y^*} = \psi(0,0) = \sqrt{\eta^2 + (a-\zeta)^2},$$
$$L_0 \equiv \varphi\big|_{y^*} = \varphi(0,0) = \sqrt{\eta_0^2 + (a-\zeta_0)^2}$$

and the incident angle

$$\gamma = \pi - (\bar{r}_{01}^{\wedge}\, \bar{n}_1) \left(\Longrightarrow \cos\gamma = \frac{\zeta_0 - a}{L_0} = \frac{\zeta - a}{L} \right),$$

we have

$$\left.\frac{\partial^2 g}{\partial y_1^2}\right|_{y=y^*} = \frac{\zeta}{aL} + \frac{\zeta_0}{aL_0} = 2\frac{\cos\gamma}{a} + \frac{1}{L} + \frac{1}{L_0},$$
$$\left.\frac{\partial^2 g}{\partial y_1 \partial y_2}\right|_{y=y^*} = 0, \tag{25}$$
$$\left.\frac{\partial^2 g}{\partial y_2^2}\right|_{y=y^*} = \frac{\zeta}{aL} + \frac{\zeta_0}{aL_0} - \frac{\eta^2}{L^3} - \frac{\eta_0^2}{L_0^3} = 2\frac{\cos\gamma}{a} + \left(\frac{1}{L} + \frac{1}{L_0}\right)\cos^2\gamma,$$
$$\det g_*'' = \left(2\frac{\cos\gamma}{a} + \frac{1}{L} + \frac{1}{L_0}\right) \cdot \left[2\frac{\cos\gamma}{a} + \left(\frac{1}{L} + \frac{1}{L_0}\right)\cos^2\gamma\right],$$

whence it is also clear, by the same reason as in the previous example, that sign $g_*'' = 2$.

On applying equation (10) with $M = 2$, $\Omega = S^+$ (the "light" part of the sphere) and $f \equiv [a^2 - (y_2\eta + y_3\zeta)]/(y_3\, \psi^2\, \varphi)$, the final result can be put in the following form ($k \to \infty$):

$$p^{sc}(x) \sim \frac{\cos\gamma\, e^{ik(L+L_0)}}{LL_0\sqrt{\left(2\frac{\cos\gamma}{a} + \frac{1}{L} + \frac{1}{L_0}\right)\left[2\frac{\cos\gamma}{a} + \left(\frac{1}{L} + \frac{1}{L_0}\right)\cos^2\gamma\right]}}. \tag{26}$$

Such a representation is to be compared with the general formula (1) given by Ray theory. In this example of reflection, the principal curvatures are $k_1 = k_2 = 1/a$, so $K = k_1 k_2 = 1/a^2$. Further, the (unit) incident ray is $\{0, -\sin\gamma, -\cos\gamma\}$, whence $\sin^2\alpha = 1$, $\sin^2\beta = \cos^2\gamma$. By substituting these values into (1), we can see that Ray-theory prediction coincides with our asymptotic solution (26). This analytic result is finally compared with a direct numerical calculation of the diffraction integral (23), for which we kept only the part of the upper half of the sphere of size $(y_1^2 + y_2^2)^{1/2} \le a/2$, see Figures 6a,b,c.

The qualitative properties pointed out for reflection from the plane screen are also valid in this example of reflection from the sphere. It is worth noting that formula (26) can be as well applied for reflection from the concave side of the sphere, by only substituting therein the value $-a$ instead of a. In such a case, there are some combinations of the geometric parameters for which the denominator vanishes, and this actually implies the well-known *focusing* effect. However, such irregular cases must be studied in a different way.

For this example of reflection, we also considered the behaviour of the phase angle of the reflected wave with respect to frequency. Of course, this behaviour is trivial in formula (26) arising from our approach (and Ray theory); what is probably worthy of mentioning is that the behaviour coming out from the numerical treatment of integral (23) is practically the same. This means that the phase is - in one sense - poorly involved in the mathematical structure of such integral, a fact which is not so evident a-priori. In Figure 6d, we show (a fragment of) such a behaviour with respect to frequency: the two lines, dashed from equation (26) and solid from equation (23), are fairly coincident; note that the interval for the phase angle is taken as $-180°, 180°$.

4. Double Reflection from Flat Surfaces

The general results expressed in equation (9a,b), (10) allow us to study multiple reflections for arbitrary curved surfaces. It is very interesting to verify whether this study will conform to the simple heuristic predictions originated from Ray theory and usually accepted by physicists in Room Acoustics, where these are applicable (see point 6 in the forthcoming Conclusions). In this connection, we now will first consider the double reflection from two plane rectangular screens S_1, S_2. To be more specific, we assume that: the ray remains on the same plane along its full path, and the reflectors form a right angle between each other; see Figure 7.

Let x_0 again denote the source point and x the receiver point; $\tilde{y}^1$ designates the first mirror reflection point and $\tilde{y}^2$ the second one. It can be easily proved that in order to provide all line segments $x_0 - \tilde{y}^1$, $\tilde{y}^1 - \tilde{y}^2$, $\tilde{y}^2 - x$ be located in the same plane, the latter one must be orthogonal to the edge between the rectangles. One thus can arrange this plane to be vertical by a simple rotation. The Cartesian coordinate system is chosen so that the plane $y_3 = 0$

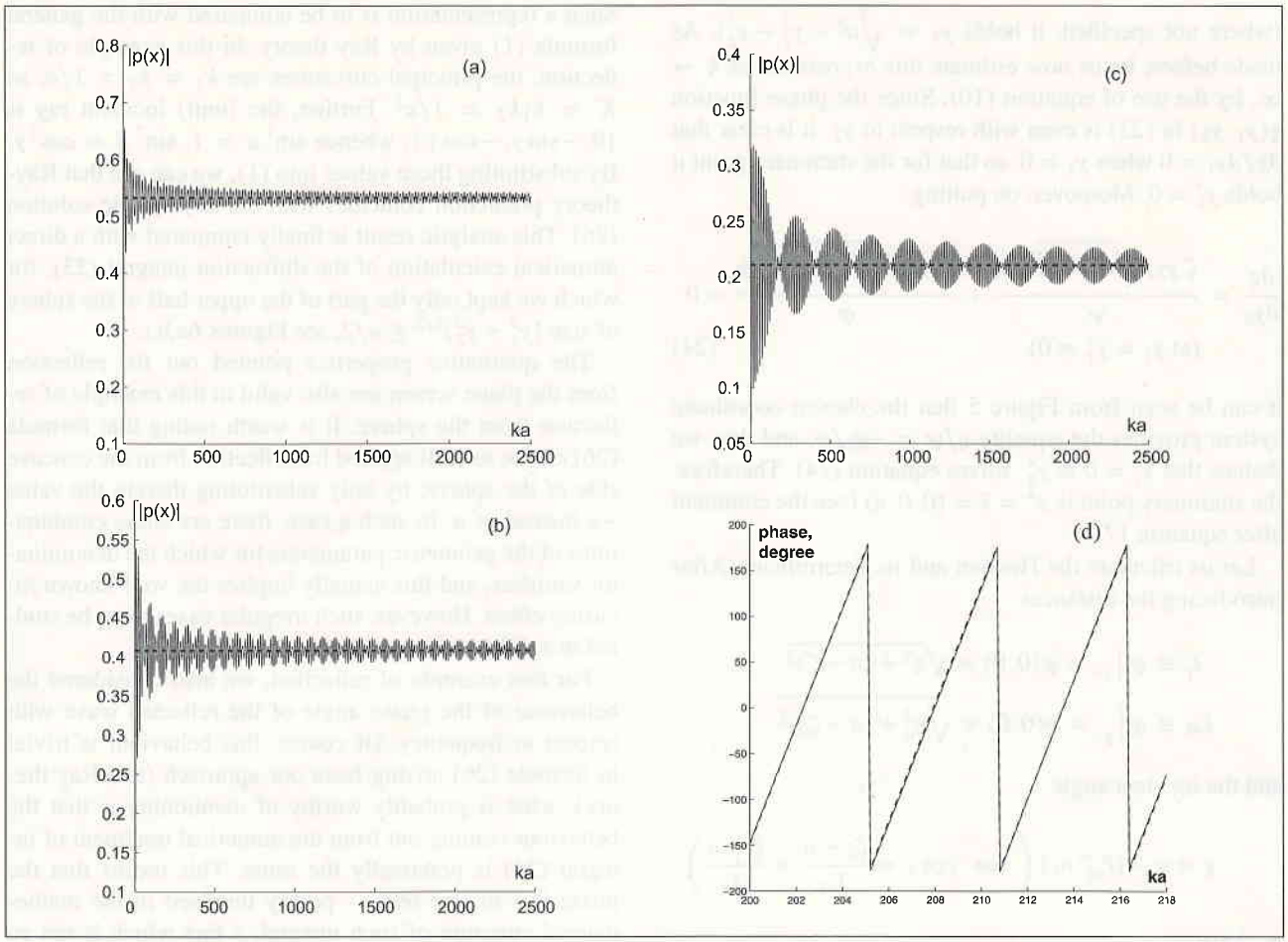

Figure 6. a,b,c. Comparison between Ray-theory prediction (26) (dashed line) and exact numerical calculation of integral (23) (solid line): spherical reflector, $\eta_0 = 0.5\,a$, $\eta = -0.5\,a$ (a): $\zeta = \zeta_0 = 1.25\,a$, $\gamma = \arctan(2) \simeq 63^o$ (b): $\zeta = \zeta_0 = 1.5a$, $\gamma = \arctan(1) = 45^o$ (c): $\zeta = \zeta_0 = 2\,a$, $\gamma = \arctan(0.5) \simeq 27^o$. (d): Comparison as above for the phase angle: spherical reflector, $\eta_0 = -\eta = 0.5\,a$, $\zeta = \zeta_0 = 1.25\,a$, $\gamma = \arctan(2) \simeq 63^o$.

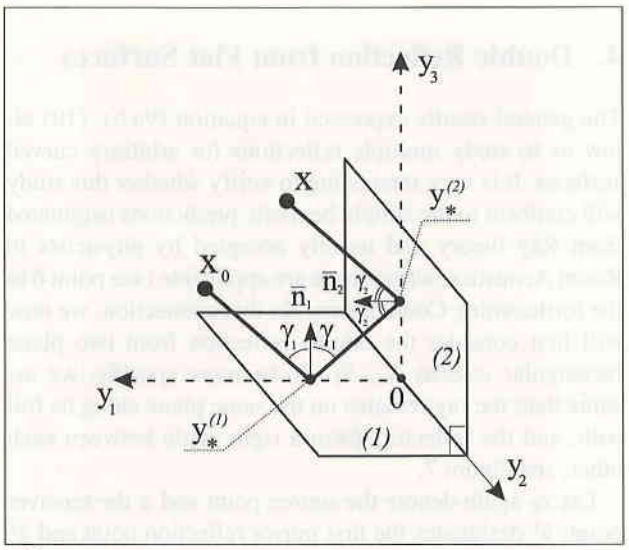

Figure 7. Double reflection from plane orthogonal rectangular screens.

is the plane of the first reflector and $y_1 = 0$ that of the second reflector. Taking suitably the origin, we can put $x_0 = (\xi_0, 0, \zeta_0)$, $x = (\xi, 0, \zeta)$. For convenience, we now denote by (ξ_i, η_i, ζ_i) the coordinates of points y^i, $i = 1, 2$; of course, it is $\zeta_1 = \xi_2 = 0$.

As a consequence, in the case at hand it holds

$$\begin{aligned} r_{01} &= \left[(\xi_1 - \xi_0)^2 + \eta_1^2 + \zeta_0^2\right]^{1/2} \equiv \varphi(\xi_1, \eta_1), \\ r_{1,2} &= \left[\xi_1^2 + (\eta_1 - \eta_2)^2 + \zeta_2^2\right]^{1/2} \equiv \mu(\xi_1, \eta_1, \eta_2, \zeta_2), \\ r_{2x} &= \left[\xi^2 + \eta_2^2 + (\zeta_2 - \zeta)^2\right]^{1/2} \equiv \psi(\eta_2, \zeta_2), \\ g &= \varphi + \mu + \psi, \\ \cos\left(\bar{r}_{1,2} \hat{} \bar{n}_1\right) &= -\frac{\zeta_2}{\mu}, \quad \cos\left(\bar{r}_{2x} \hat{} \bar{n}_2\right) = -\frac{\xi}{\psi}, \\ \mathrm{d}S_1 &= \mathrm{d}\xi_1\,\mathrm{d}\eta_1, \quad \mathrm{d}S_2 = \mathrm{d}\eta_2\,\mathrm{d}\zeta_2. \end{aligned} \tag{27}$$

Substitution of these relations into equation (9a,b) gives rise to the following formula ($k \to \infty$):

$$p^{sc}(x) \sim -\frac{k^2 \xi}{4\pi^2} \int_{S_1^+} \int_{S_2^+} \frac{\zeta_2 \mathrm{e}^{\mathrm{i}kg}}{\varphi \mu^2 \psi^2}\,\mathrm{d}\xi_1\,\mathrm{d}\eta_1\,\mathrm{d}\eta_2\,\mathrm{d}\zeta_2. \tag{28}$$

The conditions to find the stationary points $y_*^i = (\xi_i^*, \eta_i^*, \zeta_i^*)$, $i = 1, 2$:

$$\frac{\partial g}{\partial \xi_1} = 0, \quad \frac{\partial g}{\partial \eta_1} = 0, \quad \frac{\partial g}{\partial \eta_2} = 0, \quad \frac{\partial g}{\partial \zeta_2} = 0, \tag{29}$$

lead to the following 4 × 4 algebraic system

$$\frac{\xi_1-\xi_0}{\varphi}+\frac{\xi_1}{\mu}=0,\quad \frac{\eta_1}{\varphi}+\frac{\eta_1-\eta_2}{\mu}=0,$$
$$\frac{\eta_2}{\psi}+\frac{\eta_2-\eta_1}{\mu}=0,\quad \frac{\zeta_2-\zeta}{\psi}+\frac{\zeta_2}{\mu}=0. \tag{30}$$

It can be strictly proved, though not so simply, that equations (30) give $\eta_1^*=\eta_2^*=0$, as well as

$$\frac{\xi_0-\xi_1^*}{\varphi(\xi_1^*,0)}=\frac{\xi_1^*}{\mu(\xi_1^*,0,0,\zeta_2^*)},$$
$$\frac{\zeta-\zeta_2^*}{\psi(0,\zeta_2^*)}=\frac{\zeta_2^*}{\mu(\xi_1^*,0,0,\zeta_2^*)}, \tag{31}$$

which is a system to get ξ_1^* and ζ_2^*. Note that the above relations imply the reflection angles law at the stationary points $y_*^1=(\xi_1^*,0,0)=\tilde{y}^1$ and $y_*^2=(0,0,\zeta_2^*)=\tilde{y}^2$; see Figure 7.

If we introduce the distances

$$L_0\equiv\varphi(\xi_1^*,0)=\left[(\xi_1^*-\xi_0)^2+\zeta_0^2\right]^{1/2},$$
$$L_1\equiv\mu(\xi_1^*,0,0,\zeta_2^*)=\left[\left(\xi_1^*\right)^2+\left(\zeta_2^*\right)^2\right]^{1/2}, \tag{32}$$
$$L\equiv\psi(0,\zeta_2^*)=\left[\xi^2+(\zeta_2^*-\zeta)^2\right]^{1/2},$$

the components of the Hessian (at the stationary points), here a 4 × 4 matrix, are calculated as follows:

$$\left.\frac{\partial^2 g}{\partial\xi_1^2}\right|_*=\left(\frac{1}{L_0}+\frac{1}{L_1}\right)\cos^2\gamma_1,$$
$$\left.\frac{\partial^2 g}{\partial\eta_1^2}\right|_*=\frac{1}{L_0}+\frac{1}{L_1},$$
$$\left.\frac{\partial^2 g}{\partial\eta_2^2}\right|_*=\frac{1}{L}+\frac{1}{L_1}, \tag{33}$$
$$\left.\frac{\partial^2 g}{\partial\zeta_2^2}\right|_*=\left(\frac{1}{L}+\frac{1}{L_1}\right)\cos^2\gamma_2,$$
$$\left.\frac{\partial^2 g}{\partial\xi_1\partial\eta_1}\right|_*=\left.\frac{\partial^2 g}{\partial\xi_1\partial\eta_2}\right|_*=\left.\frac{\partial^2 g}{\partial\eta_1\partial\zeta_2}\right|_*$$
$$=\left.\frac{\partial^2 g}{\partial\eta_2\partial\zeta_2}\right|_*=0,$$
$$\left.\frac{\partial^2 g}{\partial\xi_1\partial\zeta_2}\right|_*=-\frac{\sin\gamma_1\cos\gamma_1}{L_1},$$
$$\left.\frac{\partial^2 g}{\partial\eta_1\partial\eta_2}\right|_*=-\frac{1}{L_1},$$

where $\gamma_1=\pi-(\bar{r}_{01}\hat{\ }\,\bar{n}_1)$ and $\gamma_2=(\bar{r}_{1,2}\hat{\ }\,\bar{n}_2)$ are the incident angles ($\gamma_1+\gamma_2=\pi/2$), so that $\cos\gamma_1=\zeta_0/L_0=\zeta_2^*/L_1$, $\cos\gamma_2=\xi/L=\xi_1^*/L_1$.

Its determinant, after some transformations, can finally be evaluated in the form

$$\Delta_4=\det g_*''=\sin^2\gamma_1\cos^2\gamma_1\left(\frac{L_0+L_1+L}{L_0L_1L}\right)^2>0. \tag{34}$$

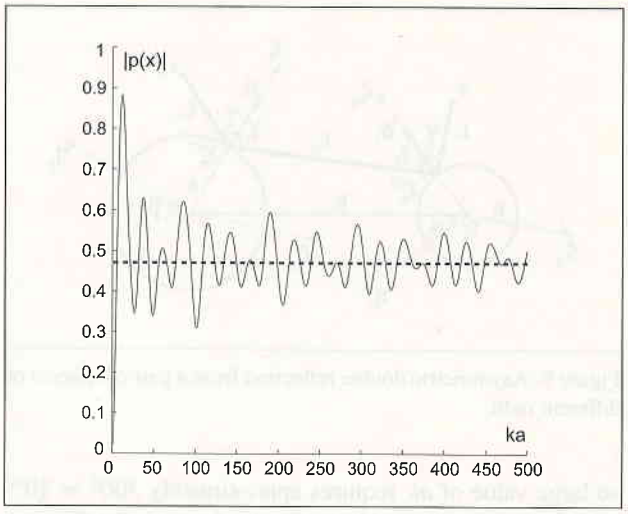

Figure 8. Comparison between Ray-theory prediction, equation (36), (dashed line) and exact numerical calculation of integral (28) (solid line) in the double reflection from $a\times a$ plane orthogonal reflectors: $x_0=(a,0,a/2)$, $x=(a/2,0,a)$, $\gamma_1=\gamma_2=45°$.

In order to obtain the sign of the Hessian, we can see that

$$\Delta_1=\left.\frac{\partial^2 g}{\partial\xi_1^2}\right|_*>0,$$
$$\Delta_2=\left.\frac{\partial^2 g}{\partial\xi_1^2}\frac{\partial^2 g}{\partial\eta_1^2}\right|_*>0, \tag{35}$$
$$\Delta_3=\left(\frac{1}{L_0}+\frac{1}{L_1}\right)\left(\frac{1}{L_0L_1}+\frac{1}{LL_1}+\frac{1}{LL_0}\right)\cos^2\gamma_1>0,$$

which implies the matrix to be positive definite; thus, sign $g_*''=4$.

The combination of (28) and (10) (with $M=4$, $\Omega=S_1^+\times S_2^+$, $f=\zeta_2/(\varphi\mu^2\psi^2)$), along with the above results, yields the following asymptotic representation for the amplitude of the doubly reflected wave field

$$p^{sc}(x)\sim\frac{\xi e^{ik(L_0+L_1+L)}}{\sin\gamma_1\cos\gamma_1\dfrac{L_0+L_1+L}{L_0L_1L}}\frac{\zeta_2^*}{L_0L_1^2L^2}$$
$$=\frac{e^{ik(L_0+L_1+L)}}{L_0+L_1+L},\qquad k\to\infty. \tag{36}$$

By comparing this result with equation (20) and the subsequent sentence, we can see that, at least in this particular example of double reflection from plane surfaces, the heuristic predictions of Room acousticians are valid.

In connection with the numerical treatment of the diffraction integral (28), whose result is shown in Figure 8 for the sake of comparison, it is useful to underline what follows: when evaluating the required number of nodes to correctly calculate the arising four-fold integral by a quadrature formula, the extremely high frequencies involved in Figure 8, like around the value $ak\sim500$, make necessary to take at least $N=300$ nodes for each of the four directions (ξ_1,η_1), (η_2,ζ_2). Hence, each one of

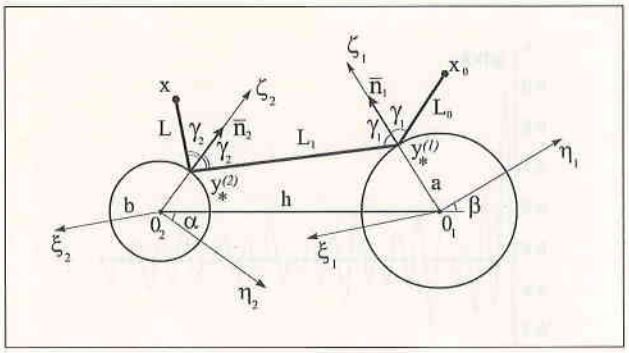

Figure 9. Asymmetric double reflection from a pair of spheres of different radii.

so large value of ak requires approximately $300^4 \approx 10^{10}$ arithmetic operations. Altogether, to construct the diagram in Figure 8, four days of continuous uninterrupted computations implemented on PC AMD-Athlon Core Due, 6.0 GHz clock frequency, were required.

Finally, it is very interesting to compare the behaviour of the reflected amplitude with respect to frequency in the two cases of single and double reflection from plane reflectors: see Figures 4a,b,c versus Figure 8. In both these cases, the (solid) oscillating line resulting from the (exact) numerical solution of the corresponding diffraction integral approaches to the (dashed) constant line reflecting Ray theory, as frequency increases. However, the oscillating behaviour for single reflection is more regular, while for double reflection is more chaotic. Physically, this may be explained in the following way. The next asymptotic term, after the leading one, is connected with the diffraction by the edges of the rectangular plate. The trajectory of the wave packet, when sliding over the edges, seems to be more regular for one reflector than for two ones, and so is the contribution of such a packet to the full pressure amplitude. Indeed, in the case of double reflection, there exist many more possible combinations of different beams which can arrive at the receiver after any passage over the edges of the two rectangular plates; hence, the contribution of such edge-diffracted waves turns out to be more chaotic with the change of frequency.

5. Asymmetric Double Reflection from a Pair of Spheres

All examples previously considered on application of the method proposed in this paper, could be (apparently) treated by this or that alternative method, even with final explicit results. Now, we give an example of double reflection which cannot be studied explicitly by any existing method known to the present authors. The reflectors are two spheres S_1 and S_2 of radius a and b, respectively; h is the distance between their centers O_1, O_2 (see Figure 9).

Like in the foregoing case, we assume all acoustic rays to be in the same plane (that of the sheet). This plane is chosen so as to contain axes η_1, η_2, ζ_1, ζ_2, the last two of which passing for the mirror reflection points $\tilde{y}^1$ and $\tilde{y}^2$, respectively; axes ξ_1, ξ_2 are clearly parallel and orthogonal to the plane. Thus, we have two coordinate systems centered in O_1 and O_2. We denote by $\tilde{\gamma}_1, \tilde{\gamma}_2$ the angles of mirror reflection from the spheres, and by α, β the angles between O_1O_2 and axes η_2, η_1, respectively; note that $\alpha + \beta = \pi - \tilde{\gamma}_1 - \tilde{\gamma}_2$.

Of course, if any point P has Cartesian coordinates ξ_1^P, η_1^P, ζ_1^P in the first system, then its coordinates in the second system are

$$\begin{aligned} \xi_2^P &= \xi_1^P, \\ \eta_2^P &= h\cos\alpha + \eta_1^P \cos(\alpha+\beta) - \zeta_1^P \sin(\alpha+\beta), \\ \zeta_2^P &= h\sin\alpha + \eta_1^P \sin(\alpha+\beta) + \zeta_1^P \cos(\alpha+\beta). \end{aligned} \tag{37}$$

It holds

$$y^1 = (\xi_1, \eta_1, \zeta_1 = \sqrt{a^2 - \xi_1^2 - \eta_1^2}),$$
$$y^2 = (\xi_2, \eta_2, \zeta_2 = \sqrt{b^2 - \xi_2^2 - \eta_2^2})$$

for points on the first or second sphere in the corresponding coordinate system. Finally, we put $x_0 = (0, \eta_0, \zeta_0)$ as coordinates of the source point in the first system and $x = (0, \eta, \zeta)$ as coordinates of the receiver in the second system.

Thus, in the case at hand we have

$$\begin{aligned} r_{01} &= \left[\xi_1^2 + (\eta_1 - \eta_0)^2 + \left(\sqrt{a^2 - \xi_1^2 - \eta_1^2} - \zeta_0\right)^2\right]^{1/2} \\ &\equiv \varphi(\xi_1, \eta_1), \\ r_{2x} &= \left[\xi_2^2 + (\eta_2 - \eta)^2 + (\sqrt{b^2 - \xi_2^2 - \eta_2^2} - \zeta)^2\right]^{1/2} \\ &\equiv \psi(\xi_2, \eta_2), \end{aligned} \tag{38a}$$

$$\begin{aligned} r_{1,2} = \Bigg\{ &(\xi_1 - \xi_2)^2 + \Big[h\cos\alpha + \eta_1\cos(\alpha+\beta) \\ &- \sqrt{a^2 - \xi_1^2 - \eta_1^2}\,\sin(\alpha+\beta) - \eta_2\Big]^2 \\ &+ \Big[h\sin\alpha + \eta_1\sin(\alpha+\beta) \\ &+ \sqrt{a^2 - \xi_1^2 - \eta_1^2}\,\cos(\alpha+\beta) \\ &- \sqrt{b^2 - \xi_2^2 - \eta_2^2}\Big]^2\Bigg\}^{1/2} \equiv \mu(\xi_1, \eta_1, \xi_2, \eta_2), \end{aligned}$$

$$g = \varphi + \mu + \psi, \qquad \mathrm{d}S_1 = \frac{a}{\zeta_1}\,\mathrm{d}\xi_1\,\mathrm{d}\eta_1,$$

$$\mathrm{d}S_2 = \frac{b}{\zeta_2}\,\mathrm{d}\xi_2\,\mathrm{d}\eta_2,$$

$$\begin{aligned} \cos\left(\bar{r}_{1,2} \overset{\wedge}{,} \bar{n}_1\right) &= (\bar{r}_{1,2}/\mu)\cdot\bar{n}_1 \\ &= (1/a\mu)\big[a^2 - \xi_1\xi_2 + h(\eta_1\cos\beta - \zeta_1\sin\beta) \\ &\quad + (\eta_2\zeta_1 - \eta_1\zeta_2)\sin(\alpha+\beta) \\ &\quad - (\eta_1\eta_2 + \zeta_1\zeta_2)\cos(\alpha+\beta)\big] \\ &\equiv f_1(\xi_1, \eta_1, \xi_2, \eta_2), \end{aligned} \tag{39}$$

$$\cos\left(\bar{r}_{2x}\hat{\ }\bar{n}_2\right) = (\bar{r}_{2x}/\psi)\cdot\bar{n}_2 = (1/b\psi)(b^2-\eta\eta_2-\zeta\zeta_2) \equiv f_2(\xi_2,\eta_2).$$

After proper substitutions, equation (9a,b) becomes

$$p^{sc}(x) \sim -\frac{k^2}{4\pi^2}\int_{S_1^+}\int_{S_2^+}\frac{f_1 f_2\, e^{ikg}}{\varphi\mu\psi}\cdot\frac{ab}{\zeta_1\zeta_2}\,d\xi_1\,d\eta_1\,d\xi_2\,d\eta_2 \quad (k\to\infty). \tag{40}$$

(where not specified, it is $\zeta_1 = \sqrt{a^2-\xi_1^2-\eta_1^2}$, $\zeta_2 = \sqrt{b^2-\xi_2^2-\eta_2^2}$).

The stationary points are defined by the following relations

$$\frac{\partial g}{\partial\xi_1} = \frac{\zeta_0\,\xi_1}{\zeta_1\,\varphi} + \frac{\xi_1\left[h\sin\beta-\eta_2\sin(\alpha+\beta)+\zeta_2\cos(\alpha+\beta)\right]-\xi_2\zeta_1}{\mu\,\zeta_1} = 0, \tag{41a}$$

$$\frac{\partial g}{\partial\xi_2} = \frac{\zeta\,\xi_2}{\zeta_2\,\psi} + \frac{\xi_2\left[h\sin\alpha+\eta_1\sin(\alpha+\beta)+\zeta_1\cos(\alpha+\beta)\right]-\xi_1\zeta_2}{\mu\,\zeta_2} = 0, \tag{41b}$$

$$\frac{\partial g}{\partial\eta_1} = \frac{\zeta_0\,\eta_1-\eta_0\,\zeta_1}{\zeta_1\,\varphi} + \frac{h(\zeta_1\cos\beta+\eta_1\sin\beta)}{\mu\,\zeta_1} + \frac{(\eta_1\zeta_2-\eta_2\zeta_1)\cos(\alpha+\beta)-(\zeta_1\zeta_2+\eta_1\eta_2)\sin(\alpha+\beta)}{\mu\,\zeta_1} = 0, \tag{41c}$$

$$\frac{\partial g}{\partial\eta_2} = \frac{\zeta\,\eta_2-\eta\,\zeta_2}{\zeta_2\,\psi} + \frac{h(\eta_2\sin\alpha-\zeta_2\cos\alpha)}{\mu\,\zeta_2} - \frac{(\eta_1\zeta_2-\eta_2\zeta_1)\cos(\alpha+\beta)-(\zeta_1\zeta_2+\eta_1\eta_2)\sin(\alpha+\beta)}{\mu\,\zeta_2} = 0. \tag{41d}$$

We can see that $\xi_1 = 0 \equiv \xi_1^*$, $\xi_2 = 0 \equiv \xi_2^*$ automatically turn (41a) and (41b) to identities. It is also obvious that $\eta_1 = 0 \equiv \eta_1^*$, $\eta_2 = 0 \equiv \eta_2^*$ convert the other two relations (41c) and (41d) to

$$-\frac{\eta_0}{\varphi} + \frac{h\cos\beta - b\sin(\alpha+\beta)}{\mu} = 0,$$
$$-\frac{\eta}{\psi} + \frac{a\sin(\alpha+\beta)-h\cos\alpha}{\mu} = 0, \tag{42}$$

which are again two identities, since both the fractions in the former give $\sin\tilde{\gamma}_1$ and both the fractions in the latter give $\sin\tilde{\gamma}_2$. Thus, the stationary points are $y_*^1 = (0,0,a) = \tilde{y}^1$, $y_*^2 = (0,0,b) = \tilde{y}^2$.

Now, after some transformations, the components of the 4×4 Hessian matrix (at the stationary points) can be written out as

$$\left.\frac{\partial^2 g}{\partial\xi_1\partial\eta_1}\right|_* = \left.\frac{\partial^2 g}{\partial\xi_1\partial\eta_2}\right|_* = \left.\frac{\partial^2 g}{\partial\xi_2\partial\eta_1}\right|_* = \left.\frac{\partial^2 g}{\partial\xi_2\partial\eta_2}\right|_* = 0,$$

$$\left.\frac{\partial^2 g}{\partial\xi_1^2}\right|_* = \frac{2\cos\gamma_1}{a}+\frac{1}{L_0}+\frac{1}{L_1},$$
$$\left.\frac{\partial^2 g}{\partial\xi_1\partial\xi_2}\right|_* = -\frac{1}{L_1},$$
$$\left.\frac{\partial^2 g}{\partial\eta_1^2}\right|_* = \frac{2\cos\gamma_1}{a}+\left(\frac{1}{L_0}+\frac{1}{L_1}\right)\cos^2\gamma_1,$$
$$\left.\frac{\partial^2 g}{\partial\eta_1\partial\eta_2}\right|_* = \frac{\cos\gamma_1\cos\gamma_2}{L_1},$$
$$\left.\frac{\partial^2 g}{\partial\xi_2^2}\right|_* = \frac{2\cos\gamma_2}{b}+\frac{1}{L}+\frac{1}{L_1},$$
$$\left.\frac{\partial^2 g}{\partial\eta_2^2}\right|_* = \frac{2\cos\gamma_2}{b}+\left(\frac{1}{L}+\frac{1}{L_1}\right)\cos^2\gamma_2, \tag{43}$$

where we introduced the distances

$$L_0 \equiv \varphi(0,0) = \sqrt{\eta_0^2+(a-\zeta_0)^2},$$
$$L \equiv \psi(0,0) = \sqrt{\eta^2+(b-\zeta)^2},$$
$$L_1 \equiv \mu(0,0,0,0) = \sqrt{a^2+b^2+h^2-2h(a\sin\beta+b\sin\alpha)-2ab\cos(\alpha+\beta)}, \tag{44}$$

and the incident angles $\gamma_1 = \pi-(\bar{r}_{01}\hat{\ }\bar{n}_1)$ and $\gamma_2 = (\bar{r}_{1,2}\hat{\ }\bar{n}_2)$, so that

$$\cos\gamma_1 = \frac{\zeta_0-a}{L_0} = \frac{h\sin\beta+b\cos(\alpha+\beta)-a}{L_1} = -\cos\left(\bar{r}_{1,2}\hat{\ }\bar{n}_1\right)\Big|_* \equiv -f_1(0,0,0,0)$$
$$\cos\gamma_2 = \frac{h\sin\alpha+a\cos(\alpha+\beta)-b}{L_1} = \frac{\zeta-b}{L} = -\cos\left(\bar{r}_{2x}\hat{\ }\bar{n}_2\right)\Big|_* \equiv -f_2(0,0). \tag{45}$$

The reflection angles law is satisfied (and of course $\gamma_1 = \tilde{\gamma}_1$, $\gamma_2 = \tilde{\gamma}_2$).

Regarding its determinant and sign, we have

$$\Delta_1 = \left.\frac{\partial^2 g}{\partial\xi_1^2}\right|_* > 0;$$
$$\Delta_2 = \left.\frac{\partial^2 g}{\partial\xi_1^2}\frac{\partial^2 g}{\partial\eta_1^2}\right|_* > 0;$$
$$\Delta_3 = \left[\frac{2\cos\gamma_1}{a}+\left(\frac{1}{L_0}+\frac{1}{L_1}\right)\cos^2\gamma_1\right]\cdot\left[\left(\frac{2\cos\gamma_1}{a}+\frac{1}{L_0}+\frac{1}{L_1}\right)\left(\frac{2\cos\gamma_2}{b}+\frac{1}{L}+\frac{1}{L_1}\right)-\frac{1}{L_1^2}\right] > 0;$$
$$\Delta_4 = \det g_*'' = \left[\left(\frac{2\cos\gamma_1}{a}+\frac{1}{L_0}+\frac{1}{L_1}\right)\left(\frac{2\cos\gamma_2}{b}+\frac{1}{L}+\frac{1}{L_1}\right)-\frac{1}{L_1^2}\right] \tag{46}$$

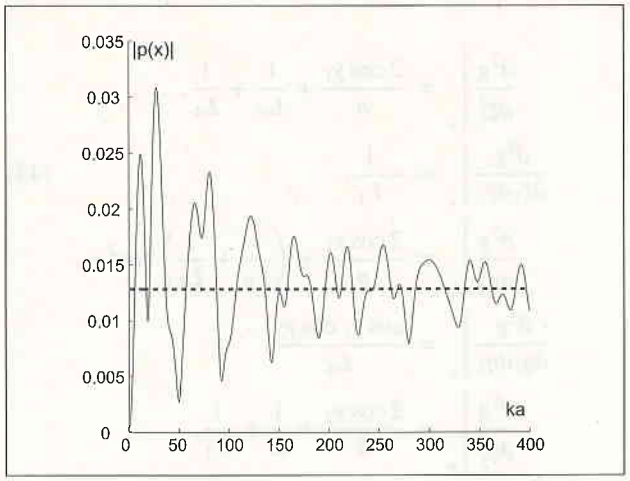

Figure 10. Comparison between asymptotic result (47) (dashed line) and exact numerical calculation of integral (40) (solid line) in the double reflection from spherical reflectors: $b = a/2$, $L_0 = L = a, L_1 = 2a$, $x_0 = (0, L_0/\sqrt{2}, a + L_0/\sqrt{2})$, $x = (0, -L/\sqrt{2}, b + L/\sqrt{2})$, $\gamma_1 = \gamma_2 = 45^o$.

$$\cdot \left\{ \left[\frac{2\cos\gamma_1}{a} + \left(\frac{1}{L_0} + \frac{1}{L_1} \right) \cos^2\gamma_1 \right] \right.$$
$$\left[\frac{2\cos\gamma_2}{b} + \left(\frac{1}{L} + \frac{1}{L_1} \right) \cos^2\gamma_2 \right]$$
$$\left. - \left(\frac{\cos\gamma_1 \cos\gamma_2}{L_1} \right)^2 \right\} > 0,$$

whence sign $g''_* = 4$.

By applying equation (10) to equation (40) (with $M = 4$, $\Omega = S_1^+ \cdot S_2^+$, $f = f_1 f_2/(\varphi\mu\psi\zeta_1\zeta_2)$), and using the above results, we finally get the following asymptotic representation for the doubly reflected amplitude:

$$p^{sc}(x) \sim \frac{\cos\gamma_1 \cos\gamma_2 \, e^{ik(L_0+L_1+L)}}{L L_1 L_0 \sqrt{\det g''_*}}, \quad k \to \infty. \qquad (47)$$

A comparison with a direct numerical treatment of the (four-fold) diffraction integral (40) is shown in Figure 10 in the case when: $b = a/2$, $\gamma_1 = \gamma_2 = \pi/4$, axis η_1 is parallel and co-directed with axis ζ_2, axis η_2 is parallel and anti-directed with axis ζ_1. It should be noted that, with integration over variables $\xi_1, \eta_1, \xi_2, \eta_2$, the phase function g varies more rapidly, so that an adequate calculation requires more grid nodes than in the case of double reflection from plane reflectors. Therefore, in order to construct Figure 10, one needs even more computation time when compared to Figure 8 (by our experience, approximately in a double time). Like in the case of a single sphere, we restricted the numerical integration to the domains with $\xi_1^2 + \eta_1^2 < (a/2)^2$, $\xi_2^2 + \eta_2^2 < (b/2)^2$.

Finally, as in the foregoing section, let us compare with each other the cases of single and double reflection for spherical reflectors: see Figures 6a,b,c versus Figure 10. The general remark that the behaviour in the double reflection is more chaotic than in the single reflection remains valid for such reflectors too. The only additional comment could be to emphasize that this irregularity is even more chaotic than for plane reflectors.

6. Conclusions

1. We have proposed a new method to estimate the leading high-frequency asymptotic term for the (complex-valued) amplitude of an acoustic wave in the multiple reflection from a set of acoustically hard surfaces. Such a method is based on a further development of the classical Kirchhoff's ideas, by extending the physical diffraction theory from single to multiple reflections. This allows us, for an arbitrary number of reflecting surfaces, to write out the amplitude at the receiving point as a multiple *diffraction integral*.
2. In the particular case of a single reflection, this integral is simply reduced to Kirchhoff's standard integral. In the case of a multiple reflection, this multi-fold integral is estimated asymptotically by means of the multi-dimensional *stationary phase* method, which gives the sought leading asymptotic term for high frequencies. We thus can see as the Ray-theory asymptotic representation is constructed on the basis of the other, namely Kirchhoff's, high-frequency theory.

   We consider some simple examples on single or double reflection only to show the basic concepts of the proposed method. Then, we consider an example of double reflection (from spherical surfaces) which cannot be studied by other known approaches, as far as the authors are acquainted.
3. The method can be well applied to reflections from both convex and concave surfaces, as soon as the geometry of the multiply re-reflected ray is calculated. The only difference between these two cases is that for convex surfaces the radii of curvature should be taken with a positive sign, while for concave surfaces – with a negative sign. One can also apply the obtained results to reflecting surfaces where two principal curvatures may be of opposite sign.
4. In principle, the Hessian determinant in the denominator of the basic asymptotic estimate (10) may vanish at the stationary point. Physically, these cases are related to concave surfaces (negative curvatures) and imply some focusing effect. Obviously, the diffraction integral (9a,b) in such cases must be estimated in an alternative way, since this typically means that the stationary point is not isolated. In the considered examples, where all curvatures are positive, we always found a strictly positive value of the principal determinant. However, this fact does not prove that a certain combination of multiple reflections from a set of convex surfaces may not yield a focusing effect. Such an interesting question requires a special study.
5. The basic Ray-theory representation is symmetric with respect to the sequence of reflections, which implies the amplitude of the multiply reflected wave to remain the same if the source and the receiver would be exchanged

in their spatial locations. One thus can see that a reciprocity principle, of general validity in acoustics, can also be stated in the problem of (high-frequency) multiple reflection from arbitrary curved surfaces.

6. In the particular case when all reflectors are flat, the calculation of the reflected amplitude is reduced to a well-known heuristic formula, which claims that this is the same as in the case of no reflection if one assumes the distance between source and receiver to be equal to the full path of the propagating ray. It should be noted that the present authors do not know any published work where such a simple idea is strictly proved as a mathematical theorem. In the present paper, we prove the above result only in the case of double reflection with the same (ray's) plane of propagation; the investigation of more general cases, though feasible in the ambit of our approach, requires some more detailed mathematical techniques, and thus is left for brevity to forthcoming studies.
7. In all the examples treated, the precision of the Ray theory (namely, of the leading asymptotic term) is estimated numerically by a direct calculation of the corresponding (multi-fold) diffraction integrals. Typically, this investigation shows a gradual approach of the numerical diagram to a constant value as predicted by the Ray theory with the frequency increasing. However, sometimes the approach reveals to occur very slowly with $k \to \infty$, and one could suppose that the second term of the full high-frequency asymptotic representation is not predicted by the Ray theory, but is defined by some contribution of the stationary points located on the boundary edges of the reflecting surfaces. This important question is also left to forthcoming studies.

Acknowledgement

The present work has been supported in part by Italian Ministry of University (M.U.R.S.T.) through its national and local projects, and in part by Russian Foundation for Basic Research (RFBR), Project 10-01-00557.

References

[1] L. B. Felsen, N. Marcuvitz: Radiation and scattering of waves. Prentice-Hall, Englewood Cliffs, New Jersey, 1973.

[2] H. Hönl, A. W. Maue, K. Westpfahl: Theorie der Beugung. Springer-Verlag, Heidelberg, 1961.

[3] H. Kutruff: Room acoustics. Applied Science, London, 1973.

[4] L. Cremer, H. A. Müller: Principles and applications of room acoustics, Vol. 1,2. Applied Science, London, 1982.

[5] E. Skudrzyk: The foundations of acoustics. Springer-Verlag, Vienna / New York, 1971.

[6] V. M. Babich, V. S. Buldyrev: Asymptotic methods in short-wavelength diffraction theory. Springer-Verlag, Berlin, Heidelberg, 1989.

[7] D. A. M. McNamara, C. W. I. Pistorius, J. A. G. Malherbe: Introduction to the uniform geometrical theory of diffraction. Artech House, Norwood, 1990.

[8] E. A. Shtager: Scattering of radio waves by obstacles of complex shape (in Russian). Radio and Communication, Moscow, 1986.

[9] Q. Wang, K. M. Li: Sound propagation over concave surfaces. J. Acoust. Soc. Amer. **106** (1999) 2358–2366.

[10] H. Ikuno, L. B. Felsen: Complex ray interpretation of reflection from concave-convex surfaces. IEEE Trans. Anten. Prop. **36** (1988) 1260–1271.

[11] H. Kuttruff: Some remarks on the simulation of sound reflection from curved walls. Acustica **77** (1992) 176–182.

[12] G. B. Deane: The beam forming properties of a concave spherical reflector with an on-axis receiver. J. Acoust. Soc. Amer. **106** (1999) 1255–1261.

[13] M. Vercammen: Reflections of sound from concave surfaces. Proc. Intern. Symp. Room Acoust. **Seville, Spain** (2007).

[14] P.-S. Kildal: Synthesis of multireflector antennas by kinematic and dynamic ray tracing. IEEE Trans. Anten. Prop. **38** (1990) 1587–1599.

[15] Y. Yamada, T. Hidaka: Reflection of a spherical wave by acoustically hard, concave cylindrical walls based on the tangential plane approximation. J. Acoust. Soc. Amer. **118** (2005) 818–831.

[16] M. A. Sumbatyan, N. V. Boyev: High-frequency diffraction by nonconvex obstacles. J. Acoust. Soc. Amer. **95** (1994) 2346–2353.

[17] R. R. Torres, U. P. Svensson, M. Kleiner: Computation of edge diffraction for more accurate room acoustics auralization. J. Acoust. Soc. Amer. **109** (2001) 600–610.

[18] M. E. Taylor: Pseudodifferential operators. Princeton University Press, Princeton, New Jersey, 1981.

[19] M. V. Fedorjuk: Stationary phase method for multiple integrals. J. Comp. Math. Math. Phys. **2** (1962) No. 1.

[20] M. Marcus, H. Minc: A survey of matrix theory and matrix inequalities. Dover, New York, 1992.